--- Supplementary Information ---

Computational Insights into the Role of Oxidation State in C–H Activation by High-Valent Iron and Manganese Oxo Oxidants

Mukhtar Ahmed[1], Sunita Srivastava[2], Ranjan Kumar Mohapatra[3], Monika[1*], Mursaleem Ansari[4*], Manoj Kumar Gupta[1*] and Azaj Ansari[1*]

[1]Department of Chemistry, Central University of Haryana, Mahendergarh – 123031, India

[2]Deparment of Physics & Astrophysics, Central University of Haryana, Mahendergarh-123031, Haryana, India

[3]Department of Chemistry, Government College of Engineering, Keonjhar-758002, Odisha, India

[4]Institut de Química Computacional i Catàlisi and Department of Chemistry, University of Girona, 17003 Girona, Spain

Corresponding authors: Monika (monika.raoji@gmail.com), Mursaleem Ansari (mansaribhu@gmail.com), Manoj Kumar Gupta (mkgupta@cuh.ac.in) and Azaj Ansari (ajaz.alam2@gmail.com)

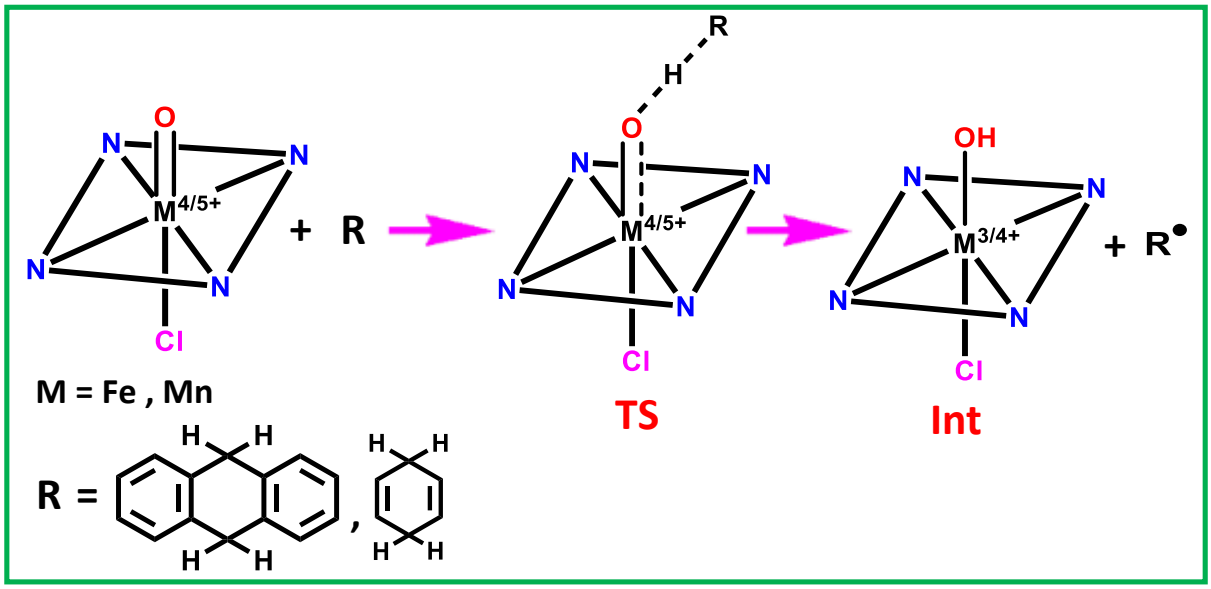

Scheme S1. Adopted mechanism for C-H bond activation using metal-oxo species.

Table S1: B3LYP computed relative energies (in kJ/mol) of oxidants, TS and intermediates.

Species	Spin states	Relative energies (in KJ/mol)	
		DHA	CHD
1	$^{5}1$	0	0
	$^{3}1$	5.9	5.9
	$^{1}1$	128.6	128.6
	$^{5}1_{HS}$-TS	84.7	78.6
	$^{3}1_{IS}$-TS	132.2	136.3
	$^{1}1_{LS}$-TS	240.2	224.6
	$^{6}1_{HS}$-INT	-67.5	-79.9
	$^{4}1_{IS}$-INT	-9.6	-21.6
	$^{2}1_{LS}$-INT	-15.3	-27.3
2	$^{4}2$	0	0
	$^{2}2$	30.7	30.7
	$^{4}2_{HS}$-TS	114.8	35.8
	$^{2}F_{LS}$-TS	50.8	81.7
	$^{5}2_{HS}$-INT	-56.7	-68.7
	$^{3}2_{IS}$-INT	-76.6	-88.6
	$^{1}2_{LS}$-INT	52.5	40.6
3	$^{4}3$	0	0
	$^{2}3$	53.5	53.5
	$^{4}3_{HS}$-TS	110.5	103.2
	$^{2}3_{LS}$-TS	165.8	155.4
	$^{5}3_{HS}$-INT	-70.3	-82.3
	$^{3}3_{IS}$-INT	-14.2	-26.1
	$^{1}3_{LS}$-INT	127.0	115.0
4	$^{3}4$	0	0
	$^{1}4$	79.6	79.6
	$^{3}4_{HS}$-TS	50.0	51.8
	$^{1}4_{LS}$-TS	186.8	174.4
	$^{4}4_{HS}$-INT	-103.4	-115.3
	$^{2}4_{LS}$-INT	52.9	40.9

Table S2. B3LYP computed structural parameters of oxidant, transition state and intermediate with substrate DHA.

	Bond length (Å)									Bond angle (º)				
Spin State	M-O	M-Cl	M-N1	M-N2	M-N3	M-N4	M-N_{avg}	O-H1	H1-C1	Cl-M-O	M-O1-H1	O-H1-C1	N1-M-N3	N2-M-N4
Species **1**; *(Fe(IV)=O)*														
^{5}**1**	1.658	2.336	2.256	2.221	2.221	2.256	2.238	-	-	177.9	-	-	173.3	173.3
^{3}**1**	1.655	2.369	2.152	2.135	2.135	2.152	2.143	-	-	178.2	-	-	175.3	175.3
^{1}**1**	1.663	2.355	2.151	2.137	2.137	2.151	2.144	-	-	178.6	-	-	175.3	175.3
Exp.[1]	1.646													
^{5}**1**$_{HS}$-TS_{DHA}	1.744	2.409	2.267	2.236	2.239	2.270	2.253	1.418	1.225	176.8	178.9	176.5	174.6	174.6
^{3}**1**$_{IS}$-TS_{DHA}	1.769	2.483	2.172	2.162	2.159	2.177	2.167	1.277	1.303	176.9	178.8	176.9	176.7	176.4
^{1}**1**$_{LS}$-TS_{DHA}	1.751	2.383	2.124	2.118	2.172	2.182	2.149	1.362	1.253	170.9	143.5	165.7	176.7	177.1
^{6}**1**$_{HS}$-INT_{DHA}	1.860	2.396	2.259	2.262	2.263	2.260	2.261	-	-	-	176.5	-	174.5	174.5
^{4}**1**$_{IS}$-INT_{DHA}	1.849	2.336	2.315	2.162	2.268	2.212	2.239	-	-	-	178.8	-	174.9	174.9
^{2}**1**$_{LS}$-INT_{DHA}	1.847	2.356	2.145	2.147	2.146	2.145	2.145	-	-	-	116.3	-	174.9	174.9
Species **2**; *(Fe(V)=O)*														
^{4}**2**	1.667	2.295	2.198	2.173	2.173	2. 198	2.185	-	-	177.9	-	-	174.2	174.2
^{2}**2**	1.658	2.237	2.141	2.156	2.156	2.141	2.148	-	-	176.3	-	-	174.6	174.6
Exp.[2]	1.679													
^{4}**2**$_{HS}$-TS_{DHA}	1.696	2.316	2.162	2.141	2.141	2.162	2.151	1.452	1.254	178.4	178.2	174.6	176.9	176.9
^{2}**2**$_{LS}$-TS_{DHA}	1.698	2.300	2.162	2.136	2.131	2.155	2.146	1.397	1.288	178.1	163.5	175.0	177.0	176.9
^{5}**2**$_{HS}$-INT_{DHA}	1.781	2.239	2.258	2.256	2.254	2.263	2.257	-	-	-	178.5	-	174.8	174.7
^{3}**2**$_{IS}$-INT_{DHA}	1.779	2.244	2.173	2.176	2.176	2.173	2.175	-	-	-	179.8	-	175.0	175.0
^{1}**2**$_{LS}$-INT_{DHA}	1.745	2.227	2.148	2.148	2.150	2.150	2.149	-	-	-	178.6	-	175.8	175.8
Species **3**; *(Mn(IV)=O)*														

^{4}**3**	1.678	2.429	2.175	2.152	2.152	2.174	2.163	-	-	177.9	-	-	175.0	175.0
^{2}**3**	1.634	2.379	2.170	2.159	2.159	2. 170	2.164	-	-	177.5	-	-	175.5	175.5
^{4}**3**$_{HS}$-TS$_{DHA}$	1.783	2.371	2.314	2.247	2.242	2.306	2.277	1.441	1.233	177.1	145.5	163.3	173.7	173.4
^{2}**3**$_{LS}$-TS$_{DHA}$	1.761	2.394	2.196	2.151	2.153	2.202	2.175	1.390	1.256	176.4	144.8	167.8	175.9	175.9
^{5}**3**$_{HS}$-INT$_{DHA}$	1.842	2.333	2.268	2.277	2.275	2.270	2.272	-	-	-	179.7	-	172.8	172.7
^{3}**3**$_{IS}$-INT$_{DHA}$	1.842	2.357	2.172	2.173	2.172	2.172	2.172	-	-	-	179.9	-	174.4	174.4
^{1}**3**$_{LS}$-INT$_{DHA}$	1.805	2.351	2.176	2.172	2.171	2.176	2.173	-	-	-	178.8	-	175.0	175.0
Species **4**; *(Mn(V)=O)*														
^{3}**4**	1.759	2.289	2.180	2.181	2.181	2.180	2.180	-	-	177.2	-	-	172.6	172.6
^{1}**4**	1.552	2.254	2.162	2.166	2.166	2.162	2.164	-	-	177.1	-	-	177.3	177.3
^{3}**4**$_{HS}$-TS$_{DHA}$	1.729	2.351	2.179	2.145	2.146	2.176	2.162	1.484	1.245	178.7	165.2	176.6	176.2	176.2
^{1}**4**$_{LS}$-TS$_{DHA}$	1.644	2.299	2.191	2.183	2.140	2.154	2.167	1.443	1.265	172.4	144.9	164.0	177.9	177.4
^{4}**4**$_{HS}$-INT$_{DHA}$	1.810	2.290	2.182	2.192	2.192	2.182	2.187	-	-	-	179.9	-	174.7	174.7
^{2}**4**$_{LS}$-INT$_{DHA}$	1.773	2.256	2.167	2.164	2.165	2.167	2.165	-	-	-	179.5	-	175.4	175.3

Table S3. B3LYP computed structural parameters of oxidant, transition state and intermediate with substrate CHD.

	Bond length (Å)									Bond angle (°)				
Spin State	M-O	M-Cl	M-N1	M-N2	M-N3	M-N4	M-N_{avg}	O-H1	H1-C1	Cl-M-O	M-O-H1	O-H1-C1	N1-M-N3	N2-M-N4
Species **1**; *(Fe(IV)=O)*														
^{5}**1**	1.658	2.336	2.256	2.221	2.221	2.256	2.238	-	-	177.9	-	-	173.3	173.3
^{3}**1**	1.655	2.369	2.152	2.152	2.135	2.135	2.143	-	-	178.2	-	-	175.3	175.3
^{1}**1**	1.663	2.355	2.151	2.137	2.137	2.151	2.144	-	-	178.6	-	-	175.3	175.3
Exp.[1]	1.646													
^{5}**1**$_{HS}$-TS$_{CHD}$	1.740	2.405	2.241	2.269	2.271	2.242	2.256	1.437	1.216	176.9	177.7	179.1	174.5	174.6
^{3}**1**$_{IS}$-TS$_{CHD}$	1.770	2.393	2.147	2.128	2.149	2.167	2.147	1.320	1.291	174.3	146.5	165.3	176.1	176.3
^{1}**1**$_{LS}$-TS$_{CHD}$	1.748	2.379	2.190	2.120	2.116	2.191	2.154	1.354	1.257	174.1	141.3	167.6	175.9	175.9
^{6}**1**$_{HS}$-INT$_{CHD}$	1.860	2.396	2.259	2.262	2.263	2.260	2.261	-	-	-	176.5	-	174.5	174.5
^{4}**1**$_{IS}$-INT$_{CHD}$	1.849	2.336	2.315	2.162	2.268	2.212	2.239	-	-	-	178.8	-	174.9	174.9
^{2}**1**$_{LS}$-INT$_{CHD}$	1.847	2.356	2.145	2.147	2.146	2.145	2.145	-	-	-	116.3	-	174.9	174.9
Species **2**; *(Fe(V)=O)*														
^{4}**2**	1.667	2.295	2.198	2.198	2.173	2.173	2.185	-	-	177.9	-	-	174.2	174.2
^{2}**2**	1.658	2.237	2.141	2.156	2.156	2.141	2.148	-	-	176.3	-	-	174.6	174.6
Exp.[2]	1.679													
^{4}**2**$_{HS}$-TS$_{CHD}$	1.698	2.294	2.224	2.270	2.260	2.229	2.245	1.428	1.264	177.5	175.7	173.5	175.5	175.6
^{2}**2**$_{LS}$-TS$_{CHD}$	1.692	2.300	2.141	2.154	2.150	2.135	2.145	1.527	1.227	176.9	167.4	173.4	177.1	177.1
^{5}**2**$_{HS}$-INT$_{CHD}$	1.781	2.239	2.258	2.256	2.254	2.263	2.257	-	-	-	178.5	-	174.8	174.7
^{3}**2**$_{IS}$-INT$_{CHD}$	1.779	2.244	2.173	2.176	2.176	2.173	2.175	-	-	-	179.8	-	175.0	175.0
^{1}**2**$_{LS}$-INT$_{CHD}$	1.745	2.227	2.148	2.148	2.150	2.150	2.149	-	-	-	178.6	-	175.8	175.8
Species **3**; *(Mn(IV)=O)*														

^{4}**3**	1.678	2.429	2.175	2.152	2.152	2.174	2.163	-	-	177.9	-	-	175.0	175.0
^{2}**3**	1.634	2.379	2.170	2.159	2.159	2. 170	2.164	-	-	177.5	-	-	175.5	175.5
^{4}**3**$_{HS}$-TS$_{CHD}$	1.780	2.365	2.303	2.244	2.247	2.311	2.276	1.488	1.210	177.1	143.7	164.3	173.2	173.5
^{2}**3**$_{LS}$-TS$_{CHD}$	1.758	2.394	2.194	2.159	2.151	2.194	2.174	1.418	1.239	176.9	144.1	165.8	175.8	175.6
^{5}**3**$_{HS}$-INT$_{CHD}$	1.842	2.333	2.268	2.277	2.275	2.270	2.272	-	-	-	179.7	-	172.8	172.7
^{3}**3**$_{IS}$-INT$_{CHD}$	1.842	2.357	2.172	2.173	2.172	2.172	2.172	-	-	-	179.9	-	174.4	174.4
^{1}**3**$_{LS}$-INT$_{CHD}$	1.805	2.351	2.176	2.172	2.171	2.176	2.173	-	-	-	178.8	-	175.0	175.0
Species **4**; *(Mn(V)=O)*														
^{3}**4**	1.759	2.289	2.180	2.181	2.181	2.180	2.180	-	-	177.2	-	-	172.6	172.6
^{1}**4**	1.552	2.254	2.162	2.166	2.166	2.162	2.164	-	-	177.1	-	-	177.3	177.3
^{3}**4**$_{HS}$-TS$_{CHD}$	1.695	2.376	2.177	2.158	2.161	2.175	2.167	2.469	1.117	177.0	167.9	157.5	176.1	176.1
^{1}**4**$_{LS}$-TS$_{CHD}$	1.641	2.289	2.195	2.188	2.142	2.149	2.168	1.409	1.274	171.5	143.4	163.0	178.1	177.4
^{4}**4**$_{HS}$-INT$_{CHD}$	1.810	2.290	2.182	2.192	2.192	2.182	2.187	-	-	-	179.9	-	174.7	174.7
^{2}**4**$_{LS}$-INT$_{CHD}$	1.773	2.256	2.167	2.164	2.165	2.167	2.165	-	-	-	179.5	-	175.4	175.3

Table S4. B3LYP computed spin density values.

Species	Spin states	Spin density values							
		DHA				CHD			
		M	**O**	**H1**	**C1**	**M**	**O**	**H1**	**C1**
1	^{5}**1**	3.092	0.631	-	-	3.092	0.631	-	-
	^{3}**1**	1.324	0.793	-	-	1.324	0.793	-	-
	^{5}**1**$_{HS}$-TS	3.728	0.239	0.011	-0.219	3.716	0.239	0.010	-0.201
	^{3}**1**$_{IS}$-TS	2.438	0.174	0.026	-0.299	1.088	0.581	-0.035	0.273
	^{6}**1**$_{HS}$-INT	4.001	-	-	-	4.001	-	-	
	^{4}**1**$_{IS}$-INT	2.914	-	-	-	2.914	-	-	
	^{2}**1**$_{LS}$-INT	1.048	-	-	-	1.048	-	-	
2	^{4}**2**	2.576	0.897	-	-	2.576	0.897	-	-
	^{2}**2**	-0.136	1.038	-	-	-0.136	1.038	-	-
	^{4}**2**$_{HS}$-TS	1.735	0.591	0.087	0.109	3.260	0.476	-0.094	-0.150
	^{2}**2**$_{LS}$-TS	0.088	0.042	0.093	0.139	-0.062	0.145	0.086	0.097
	^{5}**2**$_{HS}$-INT	3.483	-	-	-	3.483	-	-	-
	^{3}**2**$_{IS}$-INT	2.284	-	-	-	2.284	-	-	-
3	^{4}**3**	2.698	0.540	-	-	2.698	0.540	-	-
	^{2}**3**	1.155	-0.048	-	-	1.155	-0.048	-	-
	^{4}**3**$_{HS}$-TS	3.93 2	-0.485	0.022	-0.235	3.927	-0.525	0.022	-0.199
	^{2}**3**$_{LS}$-TS	1.906	-0.303	0.023	-0.258	1.904	-0.322	0.022	-0.226
	^{5}**3**$_{HS}$-INT	3.975	-	-	-	3.975	-	-	-
	^{3}**3**$_{IS}$-INT	2.060	-	-	-	2.060	-	-	-
4	^{3}**4**	3.372	-0.836	-	-	3.372	-0.836	-	-
	^{3}**4**$_{HS}$-TS	1.561	-0.240	0.092	0.108	2.905	0.206	-0.049	0.014
	^{4}**4**$_{HS}$-INT	3.424	-	-	-	3.424	-	-	-
	^{2}**4**$_{LS}$-INT	1.249	-	-	-	1.249	-	-	-

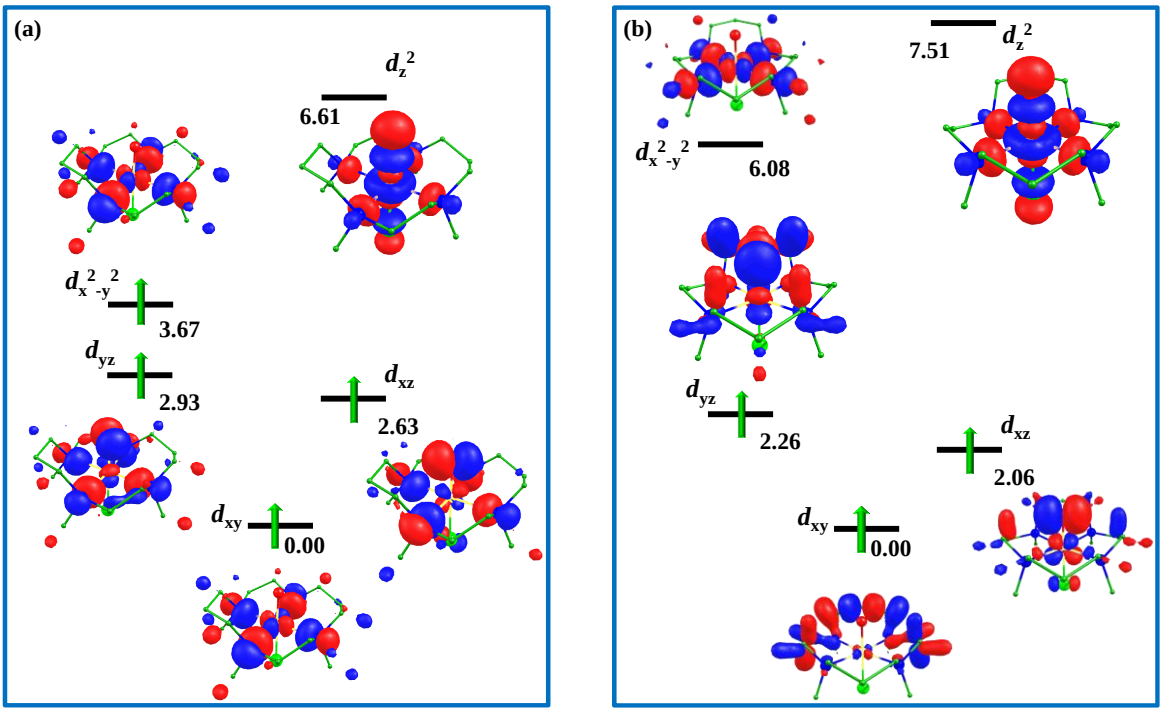

Fig. S1. Computed eigenvalue plot incorporating energies for *d*-based orbitals for alpha and beta corresponding to the ground state of a) Species **1** (^{5}**1**) and b) Species **2** (^{4}**2**) (energies are given in eV).

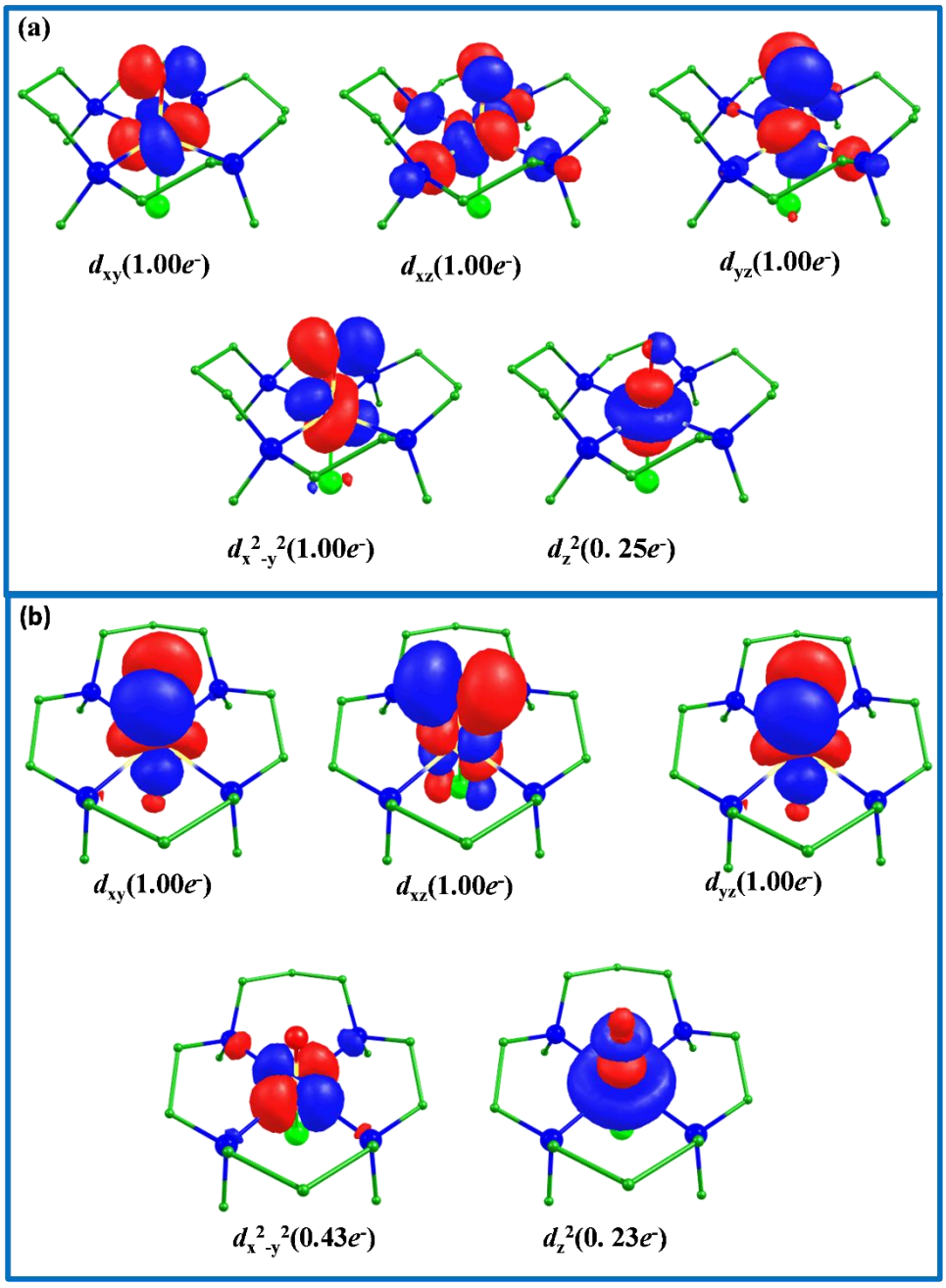

Fig. S2. Spin natural orbitals of ground state of species a) **1** (^{5}**1**) and b) **2** (^{2}**4**) (occupancy of the electron is shown in parenthesis).

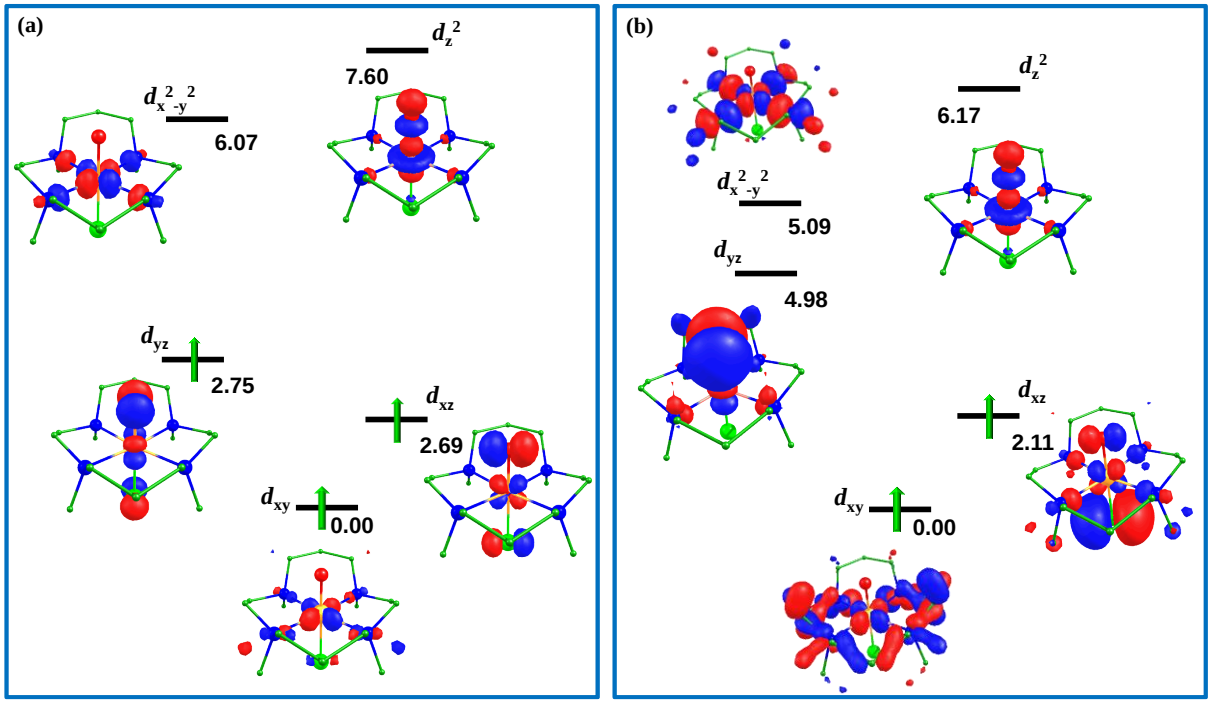

Fig. S3. Computed eigenvalue plot incorporating energies for *d*-based orbitals for alpha and beta corresponding to the ground state of a) Species **3 (^{4}3)** and, b) Species **4 (^{3}4)** (energies are given in eV).

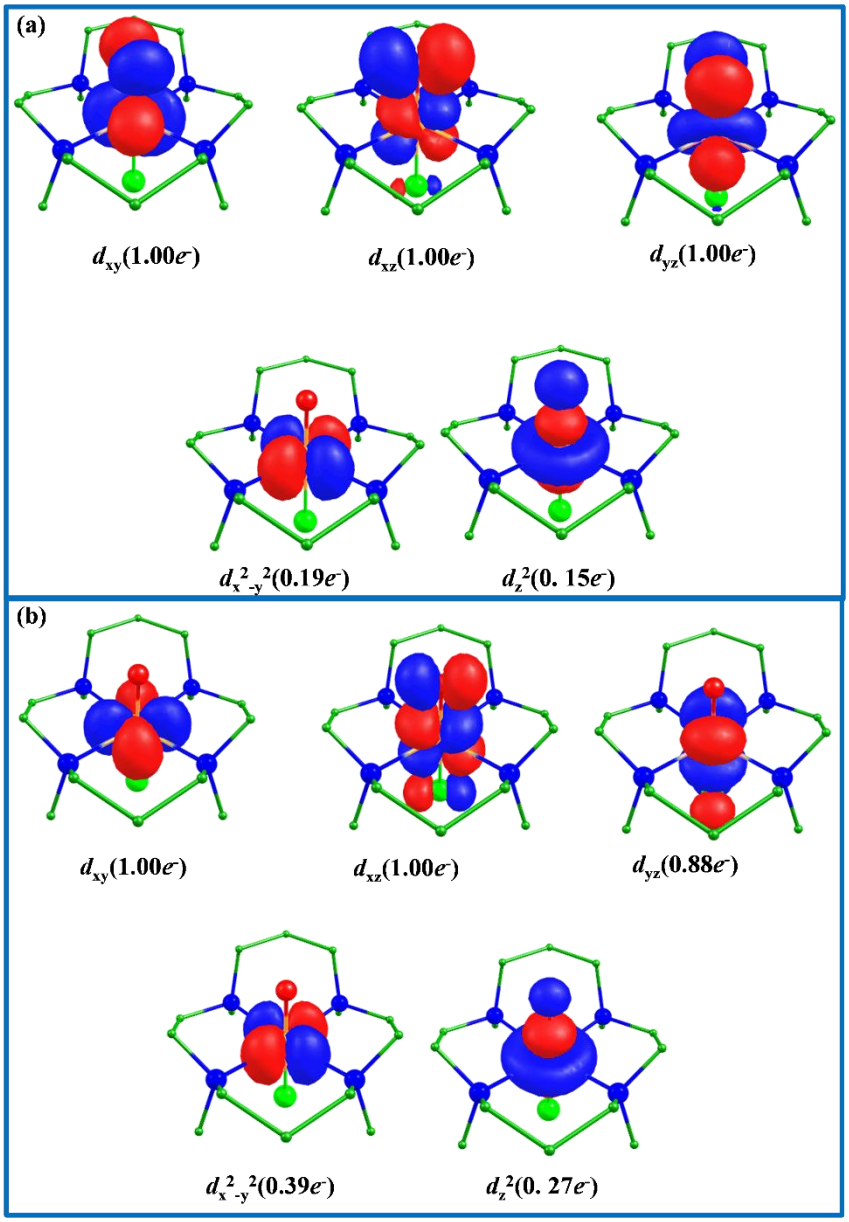

Fig. S4. Spin natural orbitals of ground state of species a) **3** (**^{4}3**) and b) **4** (**^{3}4**) (occupancy of the electron is shown in parenthesis).

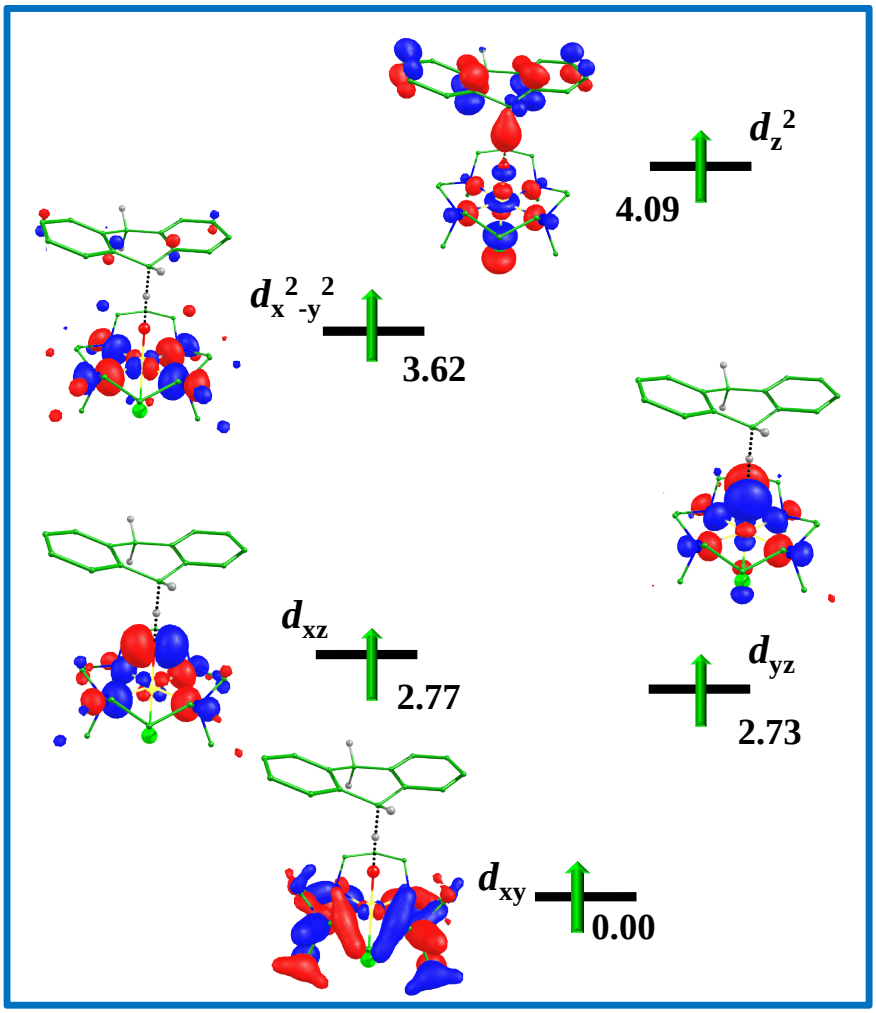

Fig. S5. Computed eigenvalue plot incorporating energies for *d*-based alpha orbitals corresponding to the ground state (^{5}1$_{HS}$-TS$_{DHA}$) transition state of C-H bond activation of DHA by species **1** (S=2; energies are given in eV).

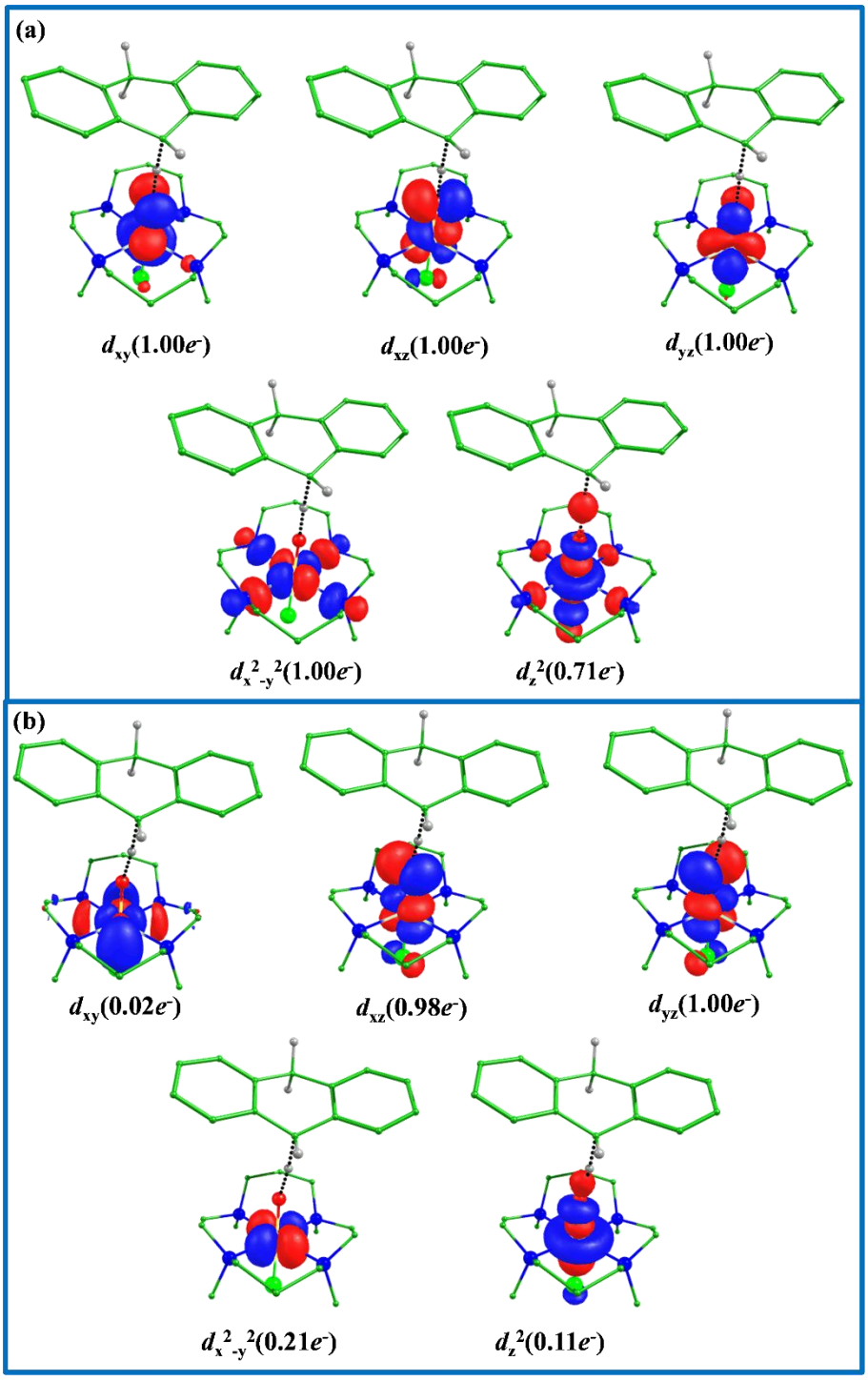

Fig. S6. Spin natural orbitals for the ground state of transition states of species a) **1** (^{5}1$_{HS}$-TS$_{DHA}$) and b) **2** (**^{2}2$_{LS}$-TS$_{DHA}$**) (occupancy of the electron is shown in parenthesis).

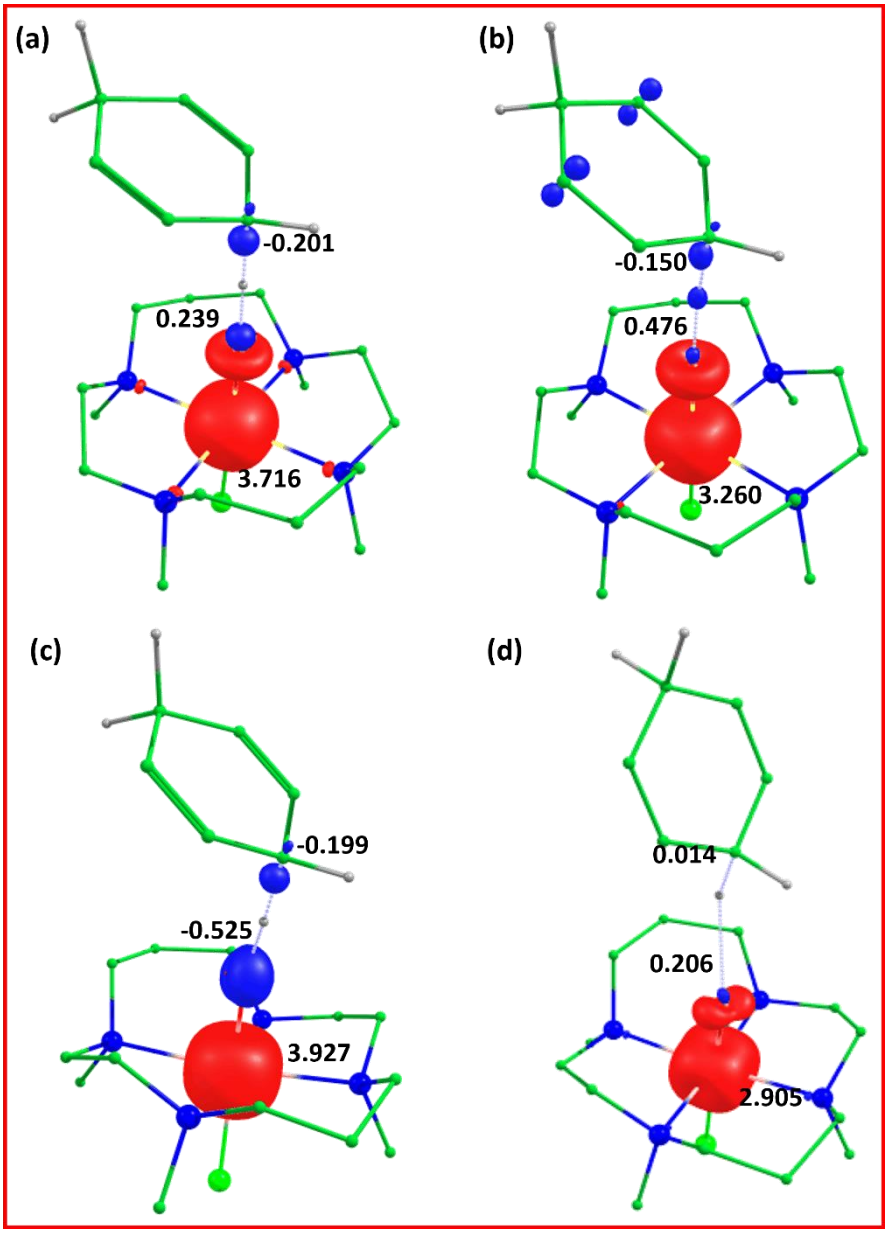

Fig. S7. B3LYP spin density plot for the ground state transition state of (a) **1** ($^{5}1_{HS}$-TS_{CHD}) (b) **2** ($^{4}2_{HS}$-TS_{CHD}) (c) **3** ($^{4}3_{HS}$-TS_{CHD}) (d) **4** ($^{3}4_{HS}$-TS_{CHD}).

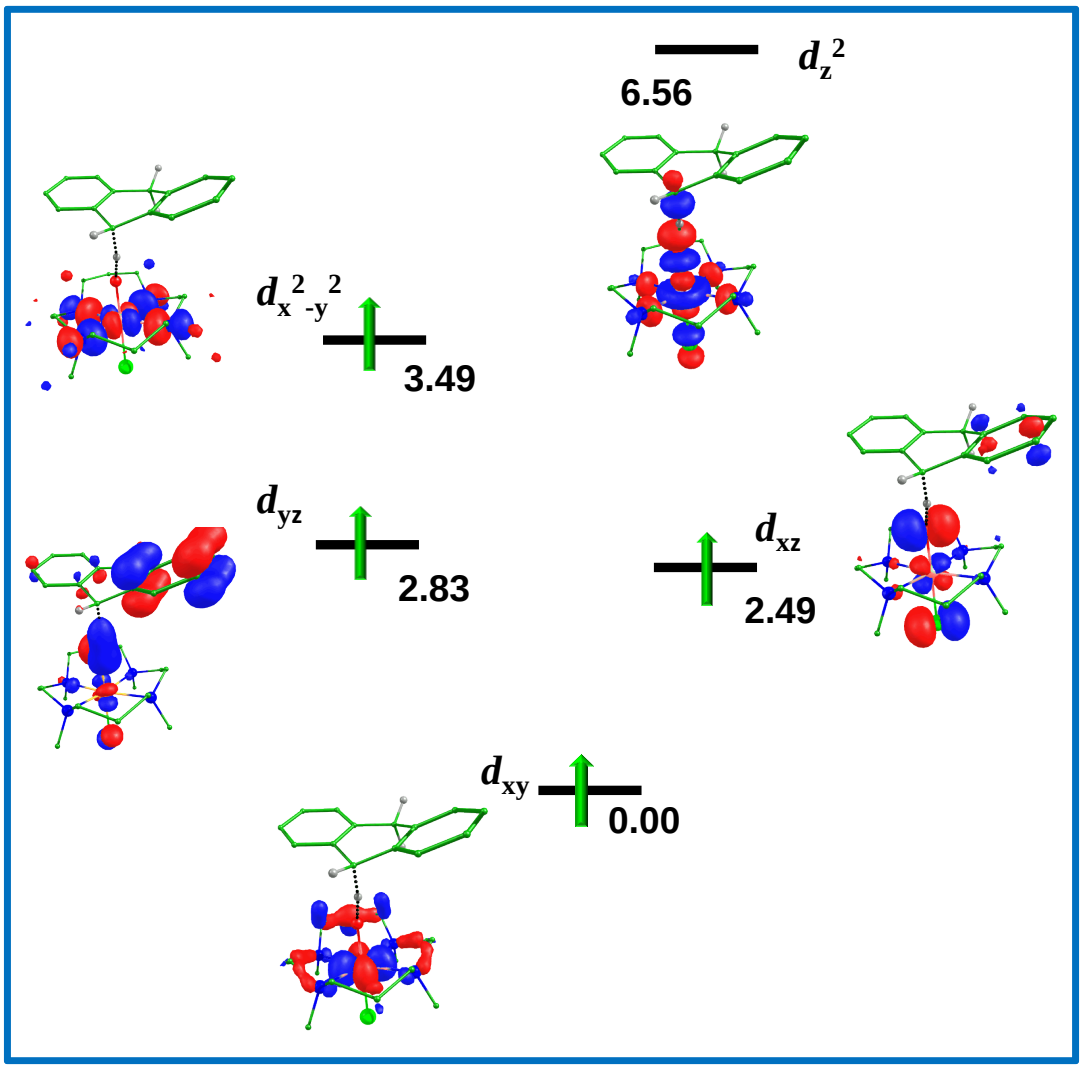

Fig. S8. Computed eigenvalue plot incorporating energies computed for *d*-based orbitals corresponding to the ground state of transition state of **3** (^{4}3$_{HS}$-TS$_{DHA}$) (energies are given in eV).

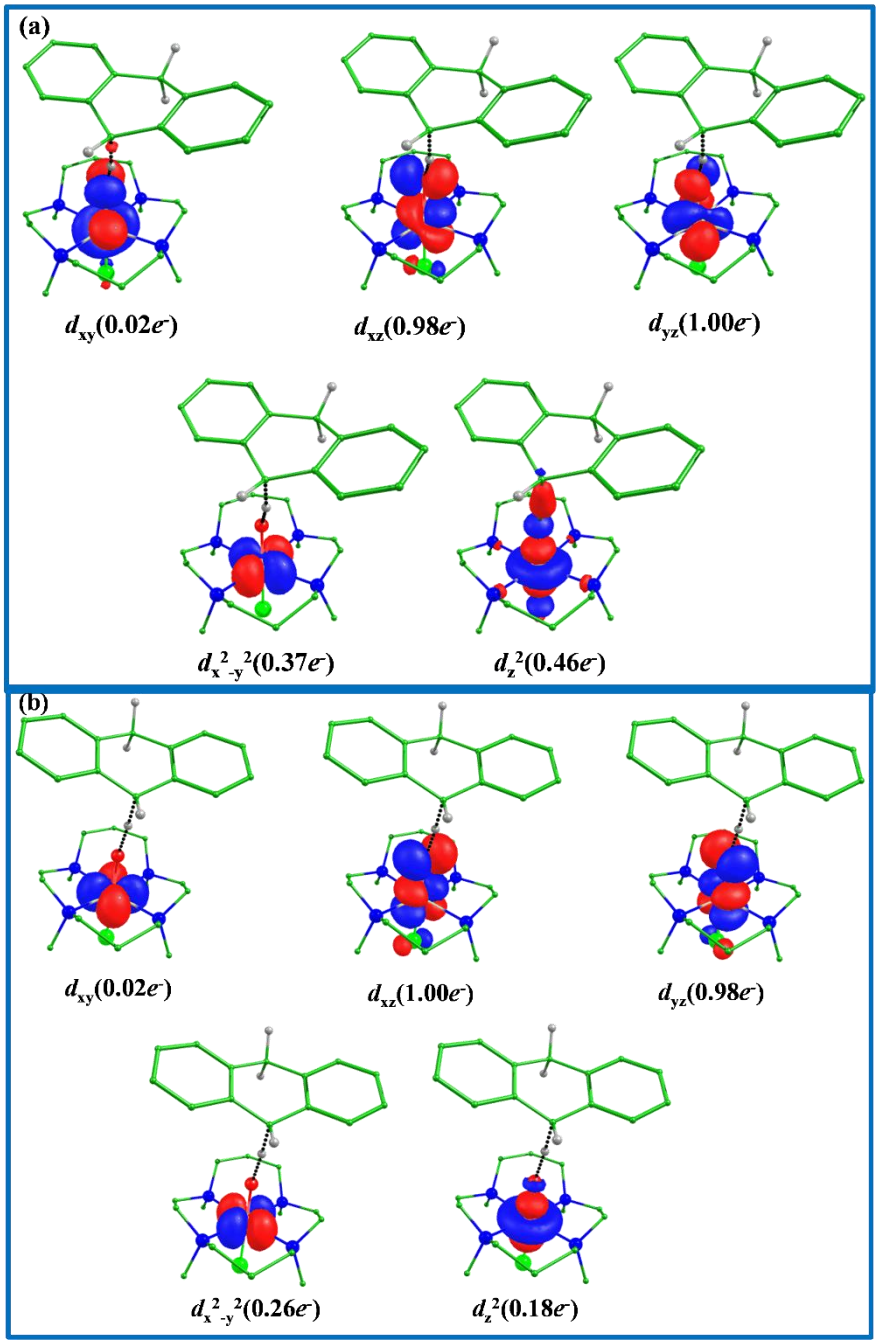

Fig. S9. Spin natural orbitals for the ground state transition state of a) **3** (^{4}3$_{HS}$-TS$_{DHA}$) and b) **4** (^{3}4$_{HS}$-TS$_{DHA}$) (occupancy of the electron is shown in parenthesis).

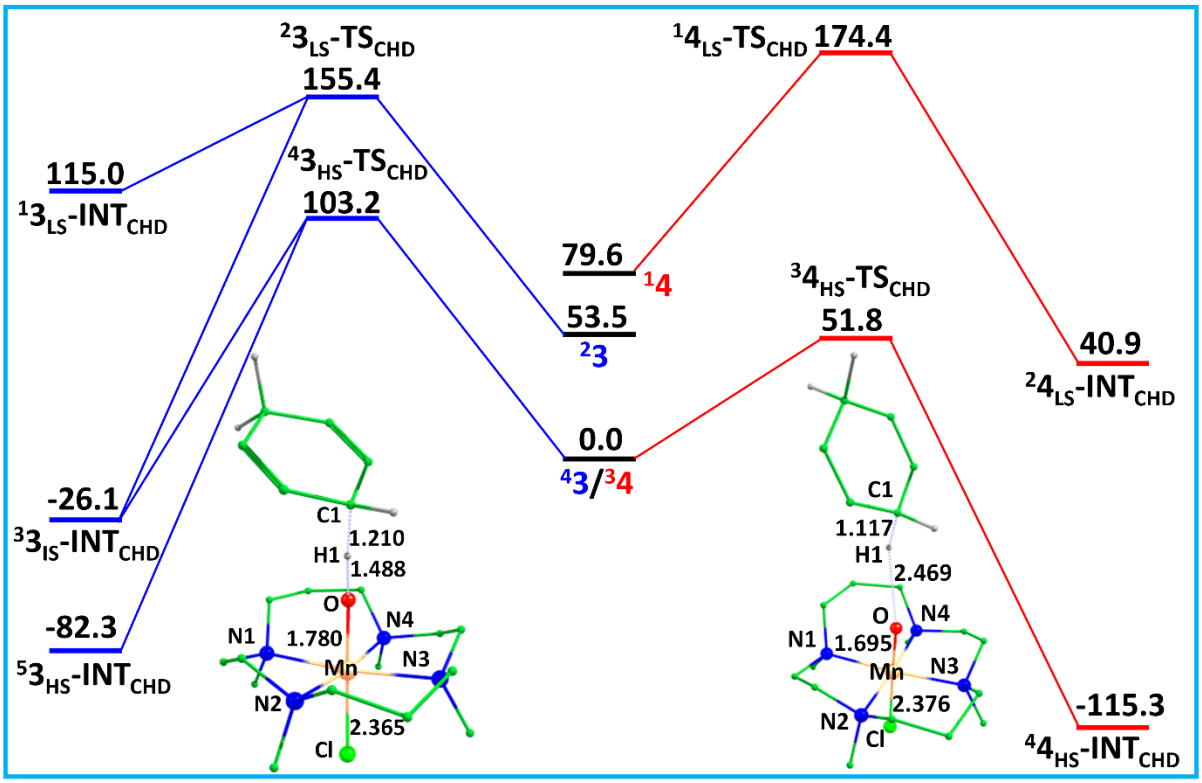

Fig. S10. B3LYP computed energy surface (ΔG in kJ/mol) for C-H bond activation of CHD by **3** (blue) and **4** (red) along with the optimized geometries of ground states of transition states, $^{4}3_{HS}$-TS_{CHD} (left) and $^{3}4_{HS}$-TS_{CHD} (right). The reaction starts in the middle and goes to the left for Mn(IV)=O **(3)** and to the right for Mn(V)=O **(4)**.

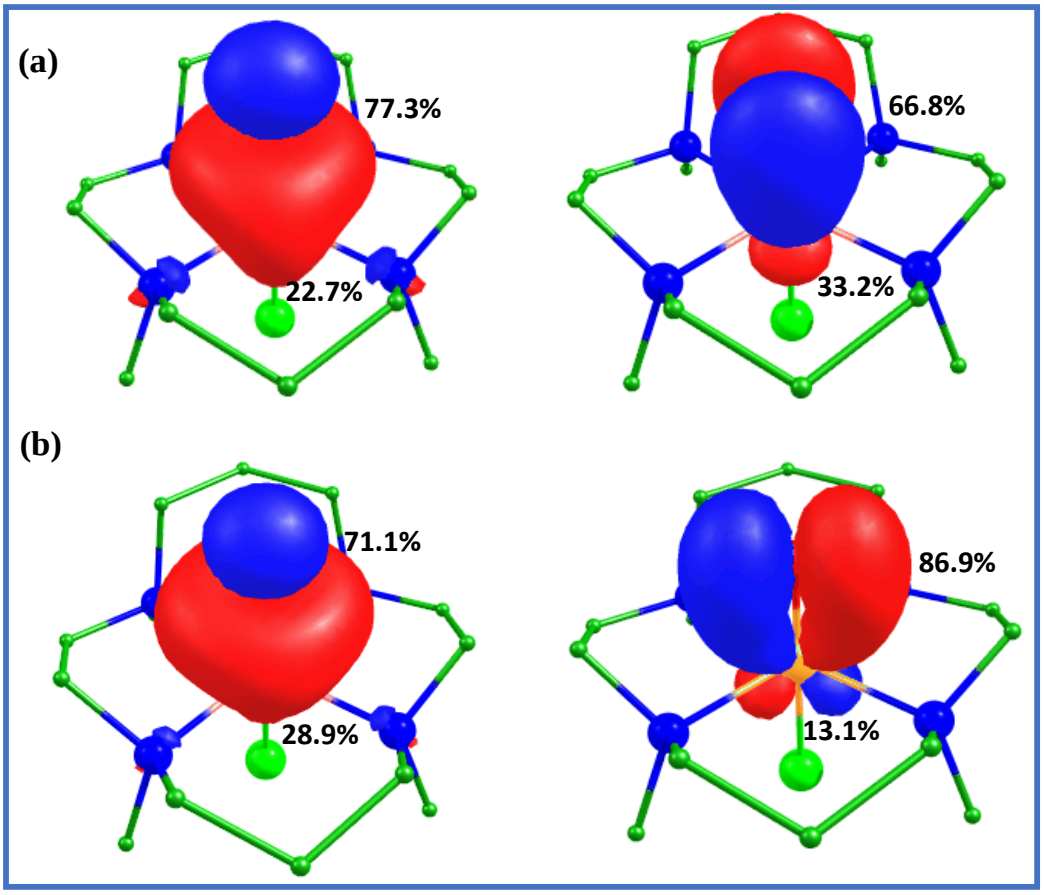

Fig. S11. Computed natural bond orbital (NBO) plots of species (a) ^{4}**3** and b) ^{3}**4**.

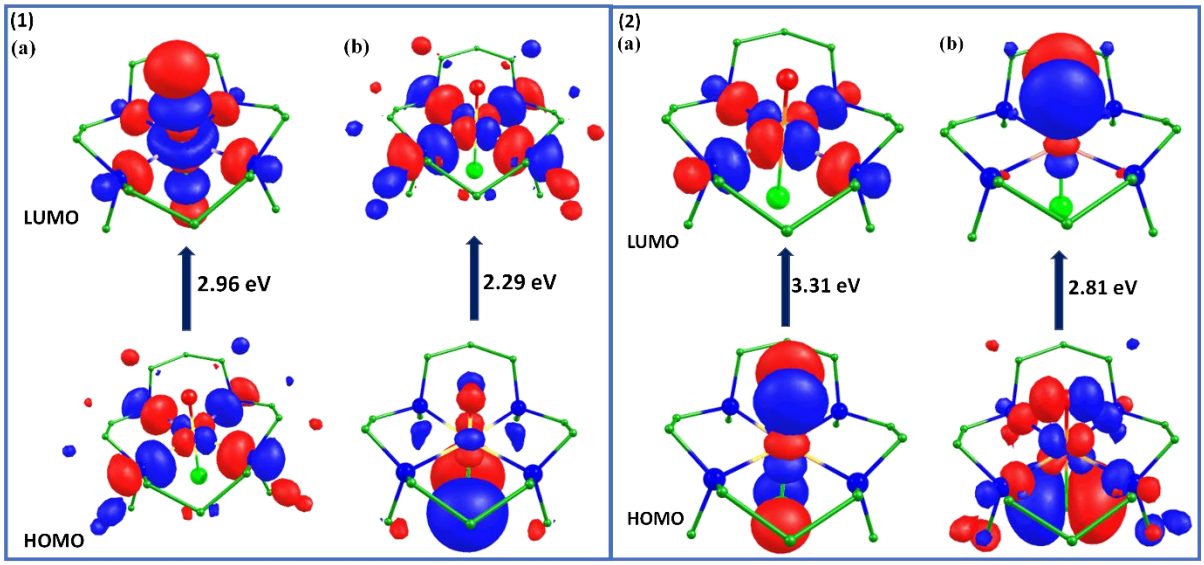

Fig. S12. Computed frontier molecular orbital of species (1a) ^{5}**1** and (1b) ^{4}**2** (2a) ^{4}**3** and (2b) ^{3}**4**.

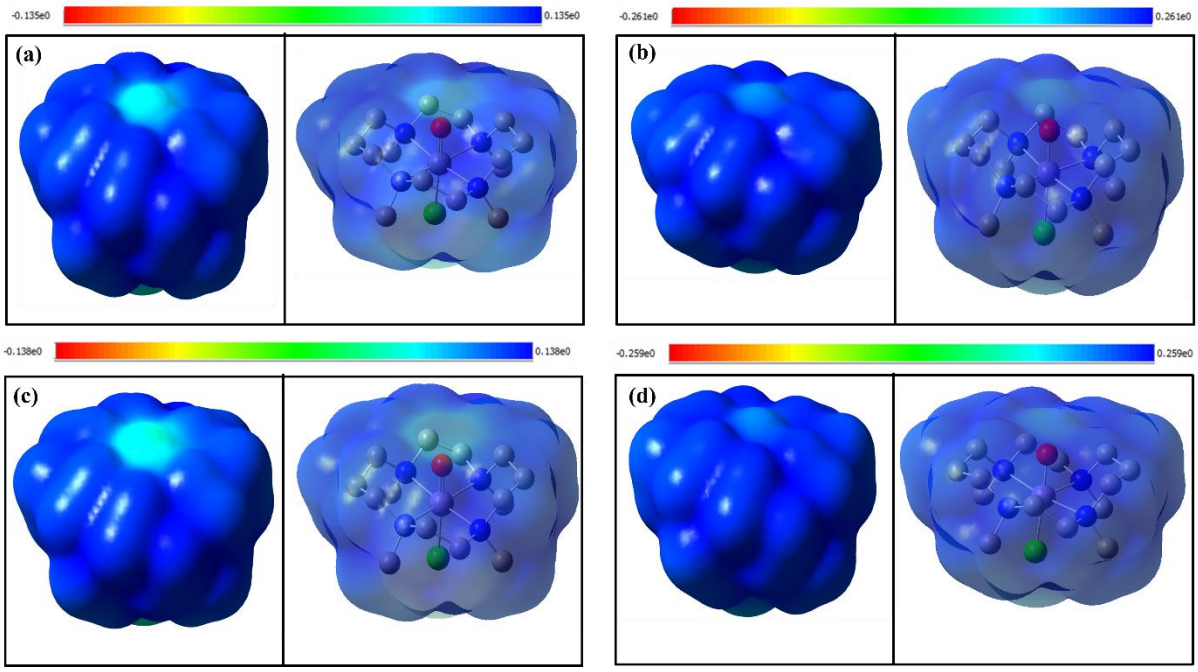

Fig. S13. B3LYP computed molecular electrostatic potential map of species (a) ^{5}**1** (b) ^{4}**2** (c) ^{4}**3** (d) ^{3}**4** (solid/transparent surface).

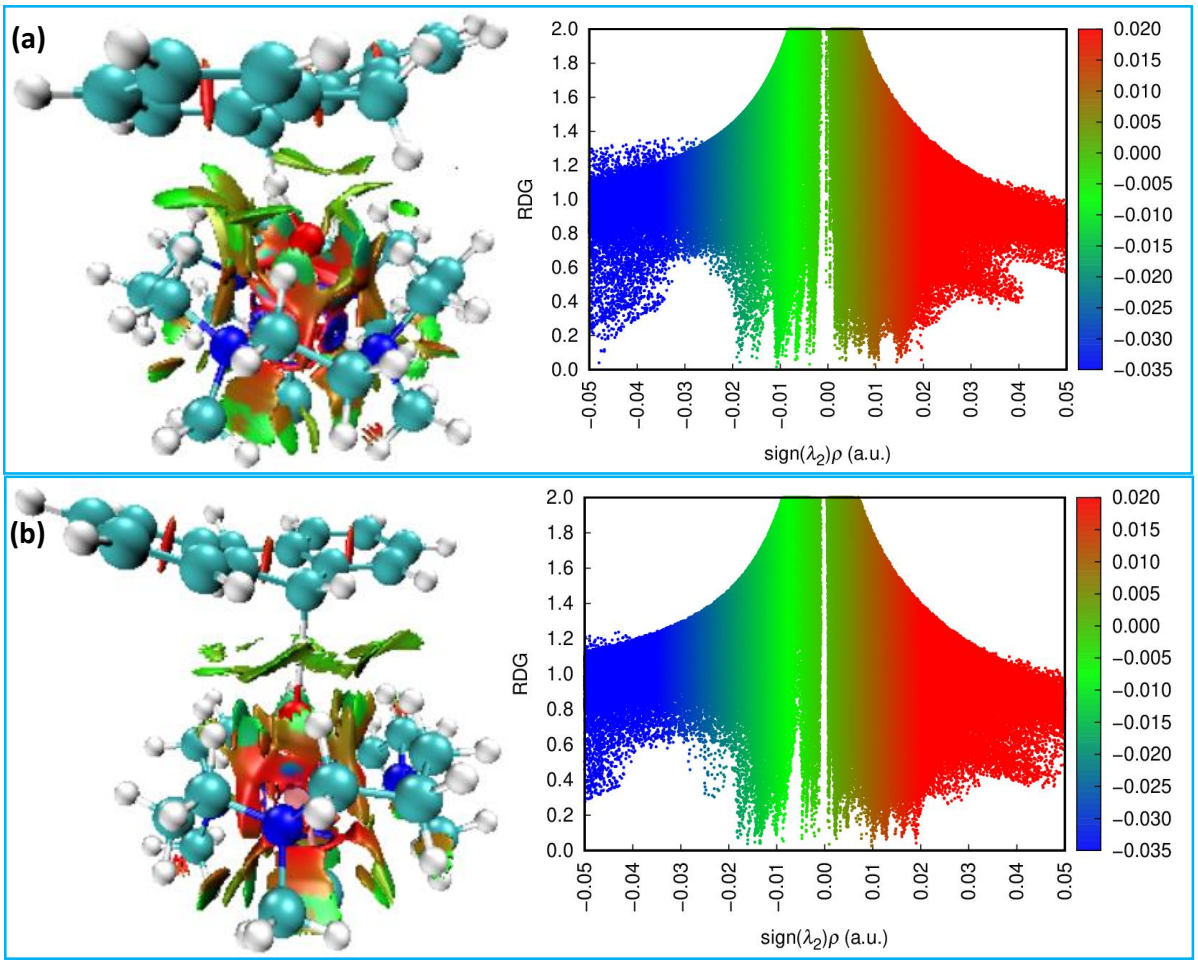

Fig. S14. NCI plots for the ground state transition state of (a) **3** (${}^{4}3_{HS}$-TS_{DHA}) (b) **4** (${}^{3}4_{HS}$-TS_{DHA}) obtained from the optimized structure where cutoffs were set at RDG(*s*) = 0.5 a.u. and -0.05 < sign(λ_2)ρ < 0.05 a.u. Colour-mapped scatter plot of RDG(*s*) as a function of sign(λ_2)ρ are shown in right side with RDG isosurface of 0.5 a.u. The color scale ranges from -0.035 a.u. (blue) to 0.020 a.u. (red); RDG: reduced gradient; λ_2: a second eigen value of electron-density Hessian matrix; ρ: electron density.

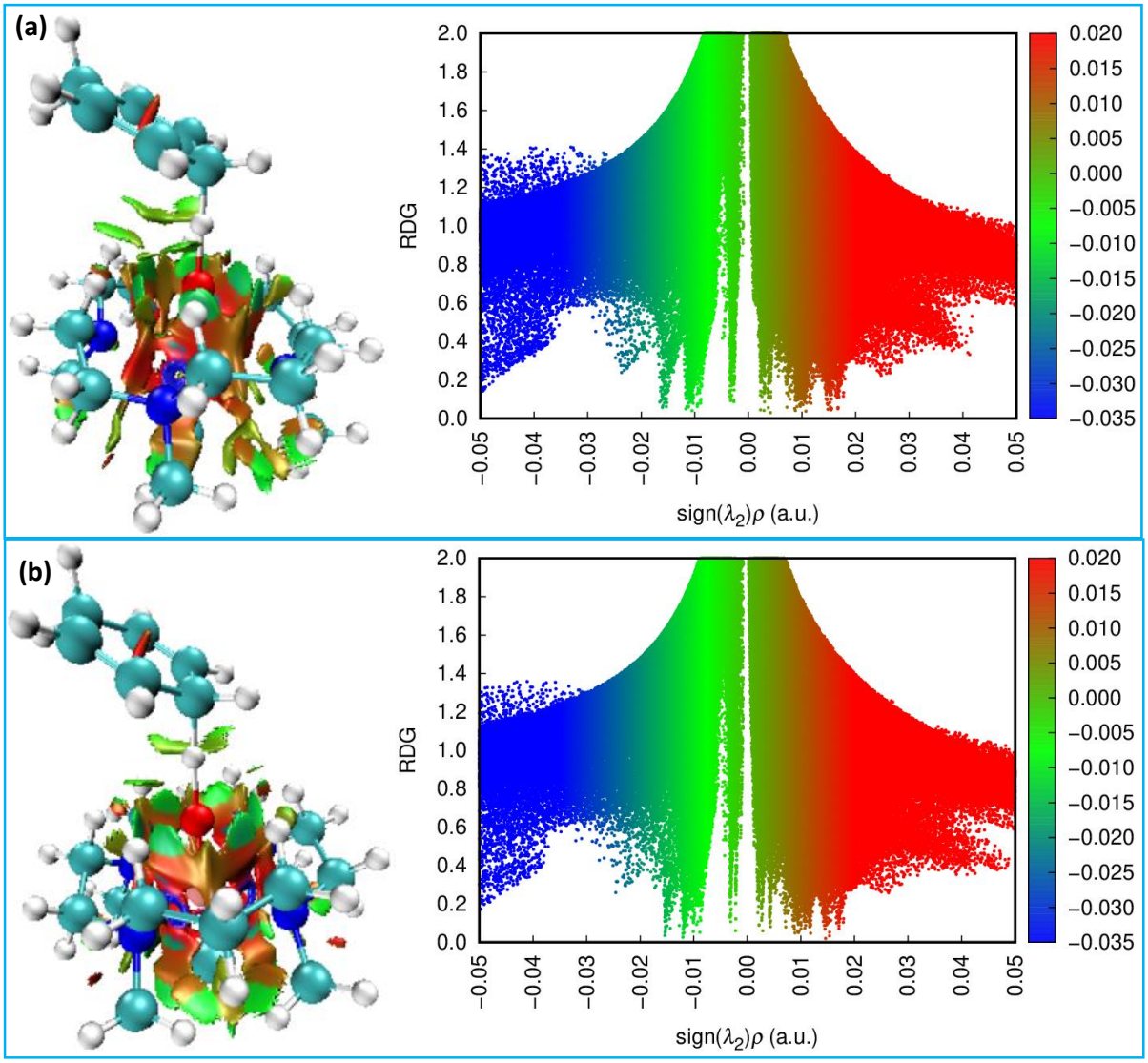

Fig. S15. NCI plots for the ground state transition state of (a) **1** (^{5}**1**$_{HS}$-TS$_{CHD}$) (b) **2** (^{4}**2**$_{HS}$-TS$_{CHD}$) obtained from the optimized structure where cutoffs were set at RDG(s) = 0.5 a.u. and -0.05 < sign(λ_2)ρ < 0.05 a.u. Colour-mapped scatter plot of RDG(s) as a function of sign(λ_2)ρ are shown in right side with RDG isosurface of 0.5 a.u. The color scale ranges from -0.035 a.u. (blue) to 0.020 a.u. (red); RDG: reduced gradient; λ_2: a second eigen value of electron-density Hessian matrix; ρ: electron density.

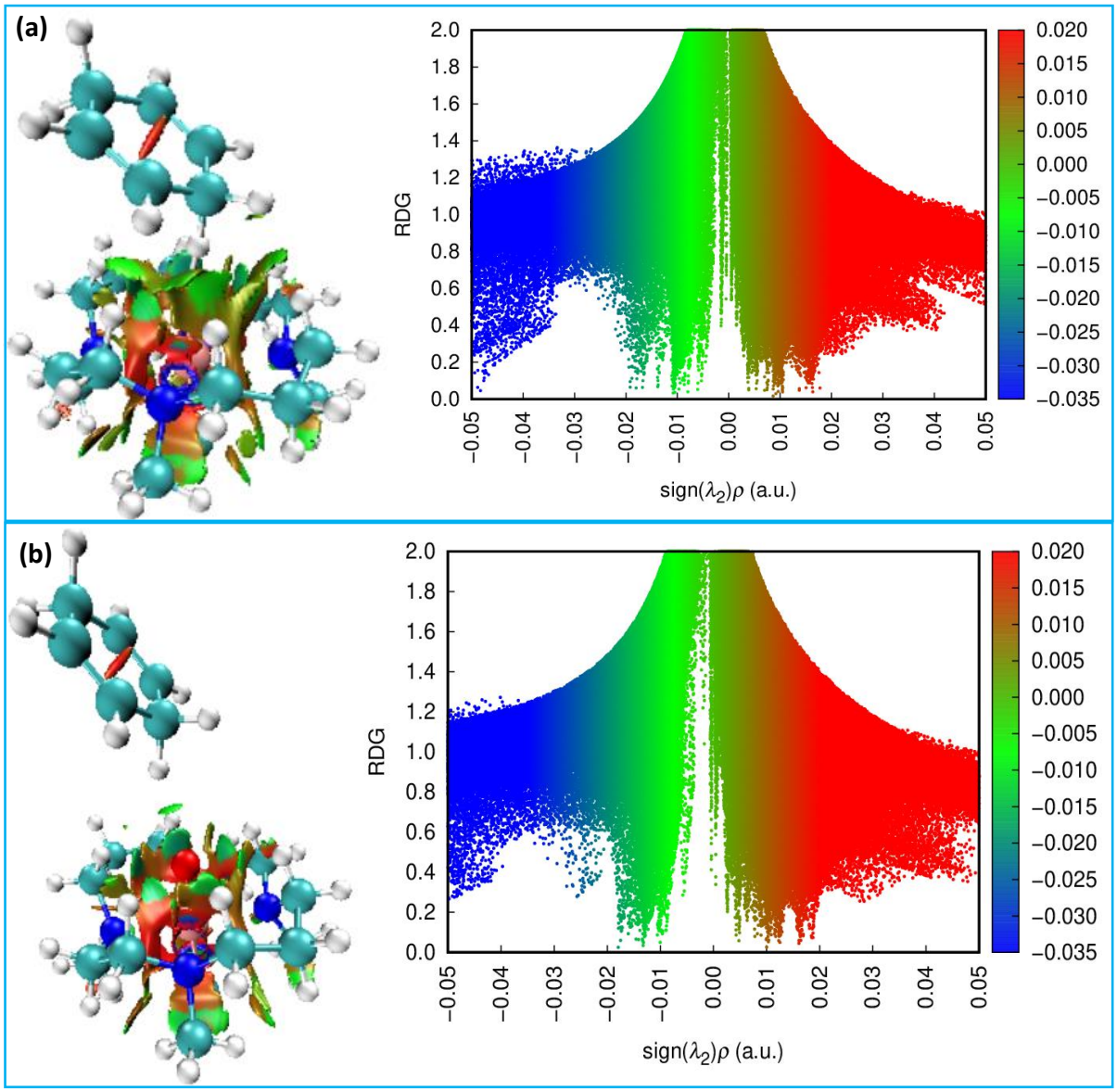

Fig. S16. NCI plots for the ground state transition state of (a) **3** ($^{4}3_{HS}$-TS_{CHD}) (b) **4** ($^{3}4_{HS}$-TS_{CHD}) obtained from the optimized structure where cutoffs were set at RDG(s) = 0.5 a.u. and -0.05 < sign(λ_2)ρ < 0.05 a.u. Colour-mapped scatter plot of RDG(s) as a function of sign(λ_2)ρ are shown in right side with RDG isosurface of 0.5 a.u. The color scale ranges from -0.035 a.u. (blue) to 0.020 a.u. (red); RDG: reduced gradient; λ_2: a second eigen value of electron-density Hessian matrix; ρ: electron density.

Table S5. Computed relative deformation energies and interaction energy in the reorganization transition states. All energies are in kJ/mol.

Species	Spin States	ΔE_{def}	ΔE_{int}	$\Delta E_{def} + \Delta E_{int}$	Barrier Height (BH)
		DHA			
1	$^{5}1_{HS}$-TS_{DHA}	35.9	48.7	84.6	84.7
2	$^{2}2_{LS}$-TS_{DHA}	55.2	-4.3	50.9	50.8
3	$^{4}3_{HS}$-TS_{DHA}	57.2	53.3	110.5	110.5
4	$^{3}4_{HS}$-TS_{DHA}	44.6	5.4	50	50.2
		CHD			
1	$^{5}1_{HS}$-TS_{CHD}	33.6	45	78.6	78.6
2	$^{4}2_{HS}$-TS_{CHD}	58.8	-22.9	35.9	35.8
3	$^{4}3_{HS}$-TS_{CHD}	51.8	51.3	103.1	103.2
4	$^{3}4_{HS}$-TS_{CHD}	17.8	33.9	51.7	51.8

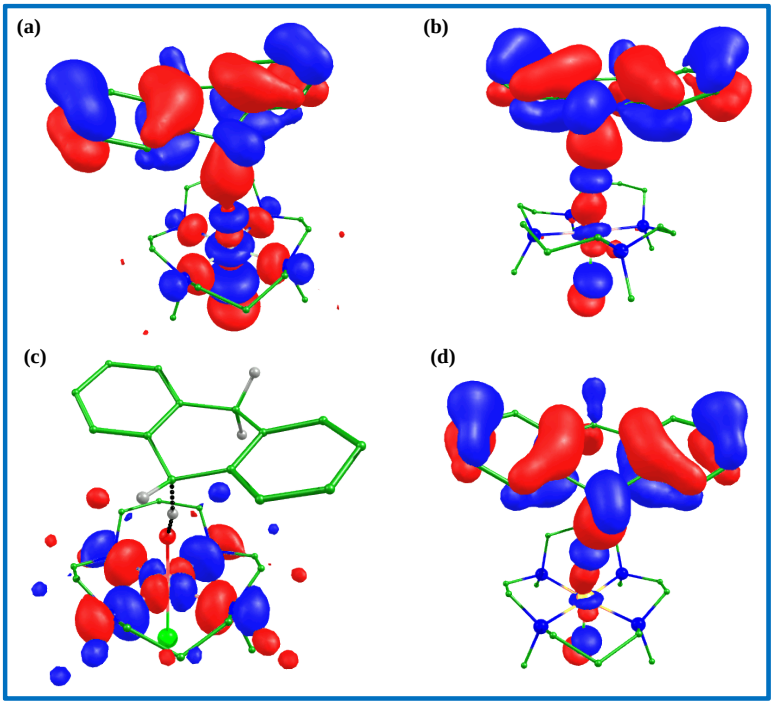

Fig. S17. B3LYP computed HOMO for the ground state transition state of (a) **1** ($^{5}1_{HS}$-TS_{DHA}) (b) **2** ($^{2}2_{LS}$-TS_{DHA}) (c) **3** ($^{4}3_{HS}$-TS_{DHA}) and (d) **4** ($^{3}4_{HS}$-TS_{DHA}).

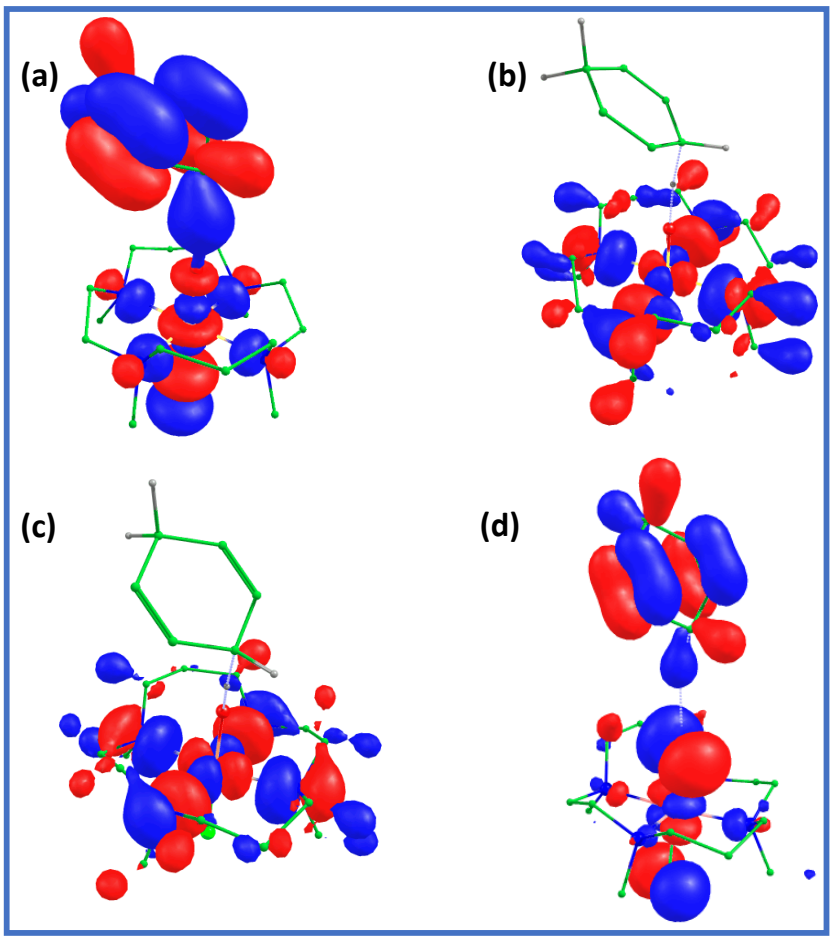

Fig. S18. B3LYP computed HOMO for the ground state transition state of (a) **1** ($^{5}1_{HS}$-TS_{CHD}) (b) **2** ($^{2}2_{LS}$-TS_{CHD}) (c) **3** ($^{4}3_{HS}$-TS_{CHD}) and (d) **4** ($^{3}4_{HS}$-TS_{CHD}).

References

1. (a) A. Karlsson, J. V. Parales, R. E. Parales, D. T. Gibson, H. Eklund, S. Ramaswamy *Science*, 2003, **299,** 1039-1042;
   (b) J.-U. Rohde, J.-H. In, M. H. Lim, W. W. Brennessel, M. R. Bukowski, A. Stubna, E. Münck, W. Nam, L. Que Jr., *Science*, 2003, **299**. 1037-1039;
   (c) J.-U. Rohde, A. Stubna, E. L. Bominaar, E. Munck, W. Nam, L. Que Jr., *Inorg. Chem*., 2006, **45** 6435-6445;
   (d) J. England, M. Martinho, E. R. Farquhar, J. R. Frisch, E. L. Bominaar, E Munck, L. Que, Jr *Angew. Chem. Int. Ed.*, 2009, **48,** 3622-3626.
2. (a) Mondal B., Neese F., Bill Eckhard, Shengfa Y. *J. Am. Chem. Soc.*, 2018, **140,** 9531-9544; (b) Monika, A. Ansari, *New J. Chem*., 2020, **44,** 19103-19112.